Title

Functional circuitry of neuro-immune communication in the mesenteric lymph node and spleen

Authors

Murray, Kaitlin
Barboza, Mariana
Rude, Kavi M
et al.

Publication Date

2019-11-01

DOI

10.1016/j.bbi.2019.08.188

Peer reviewed

HHS Public Access

Author manuscript

Brain Behav Immun. Author manuscript; available in PMC 2020 November 01.

Published in final edited form as:

Brain Behav Immun. 2019 November ; 82: 214–223. doi:10.1016/j.bbi.2019.08.188.

Functional circuitry of neuro-immune communication in the mesenteric lymph node and spleen.

Kaitlin Murray[1], **Mariana Barboza**[1], **Kavi M. Rude**[1], **Ingrid Brust-Mascher**[1], **Colin Reardon**[1,#]

[1]Department. of Anatomy, Physiology, and Cell Biology, School of Veterinary Medicine, University of California Davis, Davis, California, United States of America

Abstract

The peripheral nervous system is an active participant in immune responses capable of blocking aberrant activation of a variety of immune cells. As one of these neuro-immune circuits, the cholinergic anti-inflammatory pathway has been well established to reduce the severity of several immunopathologies. While the activation of this pathway by vagal nerve stimulation requires sympathetic innervation of the spleen, the neuro-immune circuitry remains highly controversial. Neuro-immune pathways in other lymphoid tissues such as mesenteric lymph nodes (MLN) that are critical to the surveillance of the small intestine and proximal colon have not been assessed. Using conditionally expressed Channelrhodopsin, selective stimulation of sympathetic post-ganglionic neurons in the superior mesenteric ganglion (SMG) prevented macrophage activation and LPS-induced TNFα production in the spleen and MLN, but not in the inguinal LN. Site selective stimulation of the SMG induced the release of norepinephrine, resulting in β2AR dependent acetylcholine release in the MLN and spleen. VNS-evoked release of norepinephrine and acetylcholine in the MLN and spleen was significantly reduced using selective optogenetic blockade applied at the SMG. Additionally, this optogenetic blockade restored LPS-induced TNFα production, despite VNS. These studies identify the superior mesenteric ganglion as a critical node in a neuro-immune circuit that can inhibit immune function in the MLN and the spleen.

Keywords

Neuroimmunology; Cholinergic anti-inflammatory pathway; vagal nerve stimulation; peripheral optogenetics

[#]Corresponding author: Colin Reardon, PhD, Assistant Professor, University of California, Davis, VM: Anatomy, Physiology, & Cell Biology, 1089 Veterinary Medicine Drive, VM3B, Room 2007, Davis, CA 95616, Ph: 530-752-7496, creardon@ucdavis.edu.

Author contributions:

CR conceived of the studies and planned the research. KM performed *in vivo* studies, confocal imaging, and analyzed the data. MB conducted mass spectrometry protocol development and analysis. IBM performed confocal imaging. Results were discussed by CR, KM, MB, IBM. The manuscript was written by CR with significant input from KM.

1. INTRODUCTION

The ability of the nervous system to exert regulatory control over immune cell functions has brought about not only renewed vigor in research in this field but also hope for novel therapeutic approaches to leverage these discoveries. Of the neuro-immune communication pathways, the discovery of the cholinergic anti-inflammatory pathway (CAIP) has provided not only significant insight, and new biology, but has also ushered in a number of controversies. In the CAIP, it was proposed that activation of vagal afferent sensory neurons results in activation of vagal efferent motor neuron activity, i.e. the inflammatory reflex (1–4). These efferent vagal neurons were proposed to synapse to sympathetic neurons in the celiac ganglia, with these post-ganglionic neurons innervating the spleen. Electrical vagal nerve stimulation (VNS) was proposed to use this neuroanatomical circuit to induce the release of norepinephrine (NE) followed by acetylcholine (ACh) from choline acetyltransferase (ChAT) expressing T-cells, that reduces LPS-induced macrophage activation and tumor necrosis factor (TNF)α production (3, 5). Although neuroanatomical tracing studies demonstrated vagal efferents within the celiac and superior mesenteric ganglia (SMG) (6, 7), and elegant studies showed VNS-induced immunosuppression following selective activation of vagal efferents (8), the functional circuity remains contentious. Notably, injection of the tracers fast blue in the spleen, and Dil in the dorsal motor nucleus (DMN) of the vagus did not result in co-localization within the celiac ganglia, and VNS failed to induce neural activity in the splenic nerve of the rat (9). These data suggest there is no functional circuit between the efferent vagal neurons and sympathetic innervation of the spleen in rat (9). Evidence for and against a vagal-sympathetic ganglia to spleen circuit has also been obtained using the retrograde tracer pseudorabies virus (PRV) in rats (10, 11). Despite these continued controversies, there has been an enthusiastic response and drive to leverage the CAIP in treatment of immunopathologies such as rheumatoid arthritis (12) and inflammatory bowel disease (IBD) (13).

Although the mesenteric lymph nodes (MLN) serve as the major secondary lymphoid organs where afferent lymphatics drain from portions of the small intestine and proximal colon (14), the innervation and the source of this innervation has not been thoroughly described. As in the spleen of mice, there is no definitive evidence of parasympathetic innervation of lymph nodes (15). Despite this lack of axons with ChAT immunoreactivity, B- and T-cells can act as non-neuronal sources of ACh, with sympathetic neuronal communication to ChAT $^{+}$ T-cells preventing mortality during septic shock (3, 16, 17). Our prior studies demonstrate that ChAT^{+} T-cells are present in the MLN, however the relationship and ability of the sympathetic innervation to communicate to these cells was not established (16). Although it has been proposed that a synapse-like connection occurs between sympathetic neurons and ChAT^{+} T-cells, the majority of the these cells in the spleen are not closely associated to tyrosine hydroxylase expressing (TH+), NE producing axons (17). Sympathetic innervation of the MLN has been described to be abundant in the NZW strain of mice (18) and dogs (19), entering at the hilus, wrapping vasculature, associated with medullary cords, and in the subcapsular region with fine fibers projecting to the T-cell zones. There appears to be significant differences in this abundance and patterning in different strains of mice (20) and species, including humans (21). To assess the organization of sympathetic innervation, and

the relationship between $ChAT^+$ lymphocytes and TH^+ axons in MLN, we have used confocal microscopy of MLN tissue sections from ChAT-GFP reporter mice. Although it has been proposed that lymph nodes in discrete regions receive unique afferent innervation depending on location (22), there is a significant gap in our knowledge on the origin of the sympathetic innervation in MLN.

Considering these continued controversies and knowledge gaps, we have sought to better define the functional circuitry of the MLN and spleen. To accomplish this, we have used conditional optogenetic neural stimulation or inhibition of the peripheral nervous system coupled with monitoring for NE and ACh output release by mass spectrometry, or modulation of innate immune cell activation. Using a Cre-Lox approach we have used conditional expression of the activating Channelrhodopsin2 (ChR2-YFP) or the inhibitory enhanced halorhodopsin3-YFP (eHR3-YFP) protein in Tyrosine hydroxylase expressing neurons ($Th.Cre^+$). Given the proximity of the Celiac ganglion and superior mesenteric ganglion, and the number of fibers that transit these structures, we reasoned that this highly site selective approach would be significantly better than surgical ablation. We show that optogenetic activation of cell bodies in the superior mesenteric ganglion (SMG) induce activation of the superior mesenteric neuron and prevented lipopolysaccharide (LPS)-induced TNFα production in serum, spleen and MLN but not inguinal LN. This distinction is critical as the spleen and MLN but not the inguinal LN are innervated by sympathetic neurons projecting from the SMG. Site specific stimulation further elicited NE and ACh release in the MLN and spleen. As the release of ACh from $CD4^+$ $ChAT^+$ T-cells was suggested to occur in a p2-adrenergic receptor (P2AR) dependent manner, we assessed this requirement *in vivo* by administration of the selective antagonist ICI 118 551 (23) prior to ChR2 stimulation. To determine if the SMG is part of a neuro-immune circuit that is activated by electrical stimulation of the cervical vagus, optogenetic blockade was applied directly at the SMG and significantly reduced release of NE and ACh in the spleen. These studies demonstrate that sympathetic innervation of the spleen and MLN originates in the SMG, and that specific targeting of this ganglion can be used to provide immune regulation. Together, these approaches identified that the SMG is a component of the functional neural circuit in the cholinergic anti-inflammatory reflex and could lead to activation of these processes in MLN as well.

2. Methods:

2.1 Mice:

All mice were purchased from the Jackson Labs to establish breeding colonies of the various desired genotypes. These include Th.Cre, $ChR2\text{-}YFP^{LSL}$, $eHR3\text{-}YFP^{LSL}$, ChAT-GFP reporter mice. In experiments to determine the requirement of the β2AR, mice were anesthetized using isoflurane, and the selective antagonist ICI 118 551 (1 mg/Kg), or PBS as a vehicle were i.v. injected 5 minutes prior to the start of the experiment. In optogenetic stimulation studies designed to test the importance of specific ganglia in blocking LPS-induced TNFα production, *a* midline incision was made in Th.Cre ChR2LSL mice. The ganglia were exposed, and not subjected to stimulation (Sham) or stimulated as described in

the optogenetics section. All injections of LPS were i.v., with Ultrapure LPS from E. coli 05:B5 purchased from Invivogen (San Diego, CA).

For LPS-induced TNFα production experiments with optogenetic blockade of VNS, mice were anesthetized using isoflurane and the cervical vagus nerve was exposed and a bipolar hook electrode (FHC, Bowdoin, ME) was placed. Mice were either left non-stimulated or subjected to 20 minutes of VNS (5V, 2ms, monophasic square wave, 5Hz) using a Grass stimulator S88 with a stimulus isolation module during concurrent optogenetic blockade. After 1 hour from the time of LPS injection, mice were euthanized, and cardiac puncture performed, with the serum obtained used for subsequent cytokine measurements. Nerve cuff recordings were performed in a terminal surgical procedure whereby in isoflurane anesthetized mice a midline incision was made. After the gastrointestinal tract was gently retracted the superior mesenteric artery and superior mesenteric nerve bundle were identified. A 200 μm diameter microcuff electrode (Cortec, Heidelberg, Germany) was gently placed around the nerve and artery. The electrode was electrically connected to a differential amplifier (World precision instruments, Sarasota, FL) and the output was recorded using a National Instruments DAQ using DAQexpress 2.1.0 (National instruments, Austin, TX). This DAQ device was configured to record both the trigger output signal from the optogenetic LED controller and signals from the microcuff electrode allowing for determination of when light pulse and neural activity occurred. Mice were monitored throughout the experiments by pulse-oximetry. All experimental protocols and procedures were approved by the UC Davis Institutional Animal Care and Use Committee.

2.2 Quantitative PCR

Analysis of gene expression was performed by quantitative real-time PCR (qRT-PCR) as described previously(16). Briefly, RNA was extracted from spleen, MLN, or inguinal LN, by homogenization in Trizol (Invitrogen, Carlsbad, CA) using a 5 mm stainless steel bead in a bead beater (Qiagen), according to manufacturer's instructions. Synthesis of cDNA was performed using an iSCRIPT reverse transcriptase kit (Bio-Rad, Hercules, CA), with Real time qPCR performed for the following targets using the indicated primer pairs from Primerbank (24): *Tnf* forward 5'-CCCTCACACTCAGATCATCTTCT-3', reverse 5'-GCTACGACGTGGGCTACAG-3', *Actb* forward 5'-GGCTGTATTCCCCTCCATCG-3', reverse 5'-CCAGTTGGTAACAATGCCATGT-3', *Il6* forward 5'-TAGTCCTTCCTACCCCAATTTCC-3', reverse 5'-TTGGTCCTTAGCCACTCCTTC-3'.. Amplification and data acquisition was conducted using a QuantStudio6 (Thermo Fisher Scientific, Waltham, MA). Data were analyzed using the delta CT method, normalizing gene expression to *Actb* in each sample followed by normalization to experimental control sample.

2.3 Confocal imaging

MLN with surrounding adipose and vasculature were carefully dissected, wrapped in weigh paper, placed into histology cassettes and immersed in 10% normal buffered formalin. Tissues were fixed in formalin for 24 h prior to dehydration and embedding in paraffin and cut on a microtome to produce 6 μm thick sections on slides. Slides were de-paraffinized and rehydrated according to standard protocols (17). Antigen retrieval was performed in citrate

buffer (10mM, pH 6.0, 1 h, 95°C), and slides were subjected to blocking in 5% BSA normal donkey serum (1 h, RT). Tissue sections were incubated in primary antibody overnight (16 h 4°C). Primary antibodies used in this study were rabbit Anti-TH (Millipore, AB152, Billerica, MA), goat anti-GFP (Rockland Immunochemicals, Limerick, PA), rabbit anti-TNF (Abeam, AB6671) and rat anti-CD3 (clone CD3-12, Bio-Rad, Hercules, CA). After extensive washing (3 x 5 mins), slides were incubated in appropriately labeled secondary antibodies (Invitrogen, Carlsbad, CA) for 1 h at RT, washed and mounted in Prolong gold (Invitrogen). Confocal imaging was performed on a Leica SP8 STED 3X microscope with a 63X 1.4NA objective. Areas larger than the field of view of the objective were acquired using a tiling approach, whereby adjacent images were acquired with a 10% overlap. Multiple focal planes (Z-stack) were acquired for each tile and were comprised of 20 Z-sections 0.5 μm apart. Analysis of standard confocal data sets was performed by opening Leica image format files in Imaris Stitcher (v9.0, Bitplane Scientific) to fuse overlapping fields of view together. Assessment of TNFα expression was performed on tiled confocal images of tissues of the spleen and MLN using QuPath software (25). In brief, image segmentation to identify each cell in the spleen or MLN was performed by first identifying the cell nucleus indicated by DAPI staining. Once each cell has been identified by the software, the images were assessed by manual inspection, and all files were batch-processed using these same segmentation settings. Expression of TNFα was then determined by the measuring the mean fluorescence of each identified cell. Each image tile has approximately 2000 cells.

2.4 Optogenetic stimulation and inhibition

Stimulation was performed using a computer controlled 465 nm LED light, while inhibition was achieved with a 590 nm LED light source (Plexon Inc. Dallas, TX). The light was conducted to the tissues through a fiberoptic patch cable that was held in place above the tissue of interest.

2.5 Microdialysis

Microdialysis of the spleen was performed by insertion of a probe with a 4 mm long, 20 KDa cutoff, polyarylethersulfone membrane along the longitudinal axis toward the hilus. Ringers solution (147 mM NaCI, 4 mM KCI, 2.3 mM CaCL2, pH 7.4) with 1 μM of physiostigmine bromide (Tocris) was used as the perfusate, delivered by a 1 mL gas tight Hamilton syringe, with a syringe pump (Kent Scientific, Place). Probes were washed for 5 minutes with perfusate, discarded, followed by collection of sample performed at 10 pL/min for 5 minutes. For the MLN, microdialysis probes with 2 mm in length with cupraphane membranes were used. Insertion of these devices was aided by use of a 26.5-gauge needle to pierce the outer capsule of the lymph node. Samples were collected at 5 μL/min for 5 minutes. All samples were placed on ice and frozen until analysis.

2.6 NE and ACh detection and quantification by LC-MS.

LC/MS analysis was carried out in an Agilent Infinity 1290 ultra-high-performance liquid chromatography coupled to a 6490 triple quadrupole mass spectrometer. Chromatographic separation of neurotransmitters was carried out on an Agilent Pursuit 3 Pentafluorophenyl (PFP) stationary phase (2 x 150 mm, 3 mm) column. The mobile phases were 100%

methanol (B) and water with 0.25% formic acid (A). The analytical gradient was as follows: *2%−60%* B in 2 min, 100% B from 2-4 min, 2% B for 4 min. The flow rate was 300 μl/min. Samples were held at 4°C in the autosampler, and the column was operated at 40°C. The MS was operated in positive and in selected reaction monitoring (SRM) mode. Authentic standards for NE and AcH were used to optimize instrument parameters, parent, and product ions, as well as to generate the calibration curve used for absolute quantitation. The ESI source was operated in positive ion mode, with the drying gas temperature set at 290°C and sheath gas at 375°C. The drying gas flow rate was 11 l/min and the sheath gas flow rate was 12 l/min. The nebulizer pressure was set at 35 psi. The capillary voltage was 3000 V; nozzle voltage 0 V (positive); fragmentor voltage 380 V; RF voltage for high-pressure ion funnel 150 V; and low-pressure ion funnels were 60 V (both positive and negative). Data acquisition and processing were done using Agilent Mass Hunter Qualitative Analysis (Version B.06.00) and QQQ Quantitative Analysis (Version B.08.00).

2.7 ELISA

The serum concentration of TNFα or IL-6 was determined through standard commercial sandwich ELISA assay (Thermofisher scientific Waltham, MA). In brief, 96 well maxisorp microtiter plates (NUNC, Thermofisher scientific) were coated with capture antibody, incubated with samples diluted in assay diluent, washed extensively before addition of biotin conjugated capture antibody. After incubation and extensive washing streptavidin HRP was added, incubated to allow for binding, and washed to remove unbound enzyme complex. Plates were then developed using TMB substrate with the reaction stopped by addition of 1N H_2SO_4, and optical density at 450 nm and 570 nm determined on a plate reader. Sample concentrations were determined after subtraction of blanks and 570 nm values by regression of known standard concentrations.

3. Results:

3.1 Optogenetic activation of the superior mesenteric ganglion

To determine the functional circuitry of the efferent arm of the CAIP, we performed selective stimulation of peripheral sympathetic ganglia while monitoring neurotransmitter release in the spleen and MLN. To accomplish this, mice expressing Cre recombinase under the transcriptional control of the TH promoter were crossed to mice possessing the LoxP-STOP-LoxP ChR2-YFP allele, allowing for conditional expression of YFP tagged ChR2 in TH expressing sympathetic neurons. The superior mesenteric/celiac ganglia complex was identified using anatomical landmarks including the superior mesenteric nerve (Fig. 1A). Using an epifluorescence stereomicroscope, expression of ChR2-YFP was observed in these structures and the SMN (Fig. 1B). As selective activation of the SMG in Th.Cre^+ Chr2LSL mice using illumination with a fiberoptic probe conveying 465 nm pulses of light (10 Hz, 2ms duration, square wave),was desired we first characterized the area illuminated by our fiberoptic probe. Placement of the fiberoptic parallel to a green plexiglass slide that exhibits fluorescence after excitation by 405-500 nm light revealed an illumination area of 140 μm in diameter at 250 mA power output (Fig. 1C). These results indicated that we could selectively stimulate structures that were ≥140 μm apart. We used this spatially restricted illumination for optogenetic stimulation of specific ganglia. By placing a 200 μm cuff

electrode around the superior mesenteric nerve, we observed compound action potentials evoked by optogenetic stimulation of the superior mesenteric ganglion (SMG) in Th.Cre^{+} CHR2-YFP but not Th.Cre- ChR2-YFP mice (Fig. 1D **&** S1). These evoked responses occurred only when light stimulation was applied and diminished rapidly after stimulation was terminated.

3.2 Selective stimulation of the neurons in the superior mesenteric ganglia reduce LPS-induced immune activation.

As we established that spatially restricted stimulation of the SMG could result in evoked activity in SMN, we assessed the functional impact on immune outcomes. To accomplish this, we used a previously established experimental timeline (26), where we provided sham or optogenetic stimulation of the SMG for 10 minutes prior to LPS injection, followed by another 10 minutes of stimulation with serum and tissues collected 1h after LPS (Fig 2A). In mice where the SMG was exposed but no 465 nm was delivered, LPS induced a significant increase in the concentration of serum TNFμ. In contrast mice provided optogenetic stimulation of the SMG had a significant decrease in the concentration of TNFα compared to Sham controls (Fig 2B). This inhibition was specific to ChR2 expression, as 465 nm light stimulation had no effect on mice expressing halorhodopsin-YFP (Fig. 2C). To determine if stimulation of the SMG resulted in organ specific or broad immunosuppression, we assessed TNFα transcripts in immune organs innervated (spleen, MLN) and not innervated by cell bodies in the SMG (inguinal LN) in the same mice serum was collected from. In accordance with the serum from these mice, quantitative PCR analysis revealed significantly reduced expression of TNFα in spleen and MLN from LPS + light stimulated animals compared to sham controls (Fig. 2D & E). Indicative of an effect in immune organs, light stimulation of the SMG had no effect on TNFα expression in the inguinal lymph node (Fig. 2F). Using confocal microscopy we quantified the expression of TNFα in the cells within spleen or MLN. In keeping with our ELISA and qPCR data, we observed that LPS-induced TNFα expression was significantly reduced In mice that had received optogenetic stimulation (Fig. 2G &H). This optogenetic stimulation of the SMG also significantly reduced LPS-induced serum IL-6, and expression in the spleen but not the MLN (Suppl. Fig. S2). Together our data indicate that selective stimulation of the SMG can block the activation of immune cells and consequently production of pro-inflammatory cytokines in the spleen and MLN.

3.3 Optogenetic stimulation of SMG evokes NE and ACh release in the spleen and MLN

Immune suppression in cholinergic anti-inflammatory pathway has been suggested to require sympathetic neuronal innervation of the spleen and induce the release of Ach to prevent TNFα production. With this in mind, we evaluated if stimulation of the SMG elicited NE and ACh release in MLN and spleen. Targeted stimulation of 465 nm light to the SMG induced NE and ACh release in the MLN (Fig. 3A) or the spleen (Fig. 3B). The requirement for NE to elicit ACh release following optogenetic stimulation was assessed by administration of the highly selective β2AR antagonist ICI 118 551 (23). Mice pretreated with ICI 118 551 but not the vehicle control have significantly reduced release of ACh in the MLN after optogenetic stimulation of the SMG (Fig. 3). Critically, no reduction in evoked NE in the MLN was observed in ICI 118 551 vs control mice (Fig. 3A). In the spleen, administration of ICI 118 551 prior to optogenetic stimulation of the SMG resulted in NE

release with reduced ACh release compared to vehicle controls. (Fig. 3B). Control experiments revealed that systemic administration of vehicle or ICI 118 551 alone did not significantly alter the concentration of NE or ACh in the MLN of sham mice (Fig 3C). These data indicate that axons originating from the SMG provide functional innervation to the MLN and spleen in mice, and that neuronal activation induces NE release that is required for subsequent ACh release.

3.4 Limited close interactions between ChAT$^+$ T-cells and sympathetic axons in MLN

While the sympathetic innervation of the spleen and the relationship of these fibers to ACh producing ChAT$^+$ T-cells has been described previously, the innervation of the MLN with respect to these cells has not been characterized. To determine the degree of sympathetic innervation and the relation of these axons to ChAT$^+$ T-cells, confocal microscopy was performed on MLN sections from ChAT-GFP reporter mice. In the tiled image, comprising 943 μm x 454 μm of a MLN representative of 8 ChAT-GFP mice, the TH$^+$ axons were sparse and found predominantly to the exterior of the lymph node (Fig. 4 & S3). In addition, we noted that while these fibers appear to enter at the hilus and were associated with what appear to be blood vessels, few fibers could be found near CD3$^+$ ChAT$^-$ T-cells or CD3$^+$ ChAT$^+$ T-cells. As expected from prior work, ChAT$^+$CD3$^-$ cells that appear to be B-cells, based on size and morphology, were also observed (16). We did not observe any TH$^+$ fibers in the subcapsular region, or free nerve terminals within the T-cell zone of the MLN.

3.5 Electrical VNS induces NE and ACh release in spleen and MLN through the SMG.

The functional circuitry and manner for activation of the efferent arm of the CAIP has proved highly contentious. We sought to address if the SMG is a component in the CAIP by using a combination of electrical stimulation and spatially restricted optogenetic blockade to achieve selective blockade of sympathetic post-ganglionic neurons that innervate the spleen and MLN. To accomplish this, mice expressing Cre under the control of TH promoter were crossed to mice encoding a LoxP-STOP-LoxP enhanced halorhodopsin-YFP cassette. The resulting progeny of this cross express eHR3-YFP in TH expressing neurons, allowing for targeted blockade of neuronal signaling in these neurons. As expected, electrical stimulation of the cervical vagus nerve (5 V, 2 ms, monophasic square wave, 5 Hz) induced release of NE and ACh in the spleen (Fig 5A) and MLN (Fig 5B). This VNS-evoked increase in neurotransmitters was significantly reduced in the MLN by optogenetic blockade applied by delivering 590 nm pulses of light (10 Hz, 2 ms duration, square pulses) to the SMG concurrent to electrical cervical VNS. These data demonstrate that neurons in SMG can serve as part of the functional circuitry activated by electrical VNS to cause effects in the spleen and MLN. Additionally, in a model of septic shock, TH Cre$^+$ eHR3-YFP mice were challenged with LPS and subjected to either VNS only or VNS accompanied by optogenetic blockade. Mice not receiving electrical VNS or optogenetic block had the respective region surgically exposed in the sham treatment (Fig 5C).

As expected from the literature, electrical VNS significantly lowered serum LPS-induced TNFα production compared to mice injected with LPS. Optogenetic blockade applied to the SMG during VNS impeded the anti-inflammatory effects of VNS and resulted in serum TNFα production that was significantly increased compared to naive, and LPS + VNS

treated mice (Fig 5D). This optogenetic blockade during VNS was able to restore LPS-induced TNFα production to approximately 50% of the LPS sham VNS treatment group. These data suggest the importance of the SMG as part of the neuro-immune regulatory circuit induced by electrical VNS.

4. Discussion:

Over the course of the past two decades there has been a resurgence in interest in the ability of the nervous system to control immune cell activation. This renewed interest is due to key studies demonstrating that VNS can reduce aberrant immune activation in a diverse number of settings. These include reduced production of pro-inflammatory cytokines during models of septic shock (3), rheumatoid arthritis (27), and ischemia and reperfusion induced renal injury (28–30). While there is substantial evidence that neuronal modulation of aberrant immune cell activation in these models requires neuro-immune communication in the spleen, other anatomical sites of action have been identified. VNS-mediated blockade of immunopathology in models of IBD has been proposed to occur by direct vagal efferent modulation of immune cells in the intestinal tract (31). This direct innervation of the intestine by vagal efferents is however limited to small intestine and proximal colon in most species, with sparse axons present beyond the mid-distal colon (32). With this in mind, immunomodulation throughout the Gl tract would appear to require additional functional circuits.

Mesenteric lymph nodes function as inductive sites where dendritic cells (DC) sampling antigen from the small intestine and proximal colon migrate to present antigen to T-cells in health and disease (33–35). As such, these lymph nodes are of significant importance in the development of mucosal immune responses during homeostasis and responses to enteric pathogens (36, 37). Despite this wealth of knowledge, the innervation, and ability of the innervation in the lymph nodes to alter immunological outcomes was largely unknown. Our studies set out to reduce this gap in knowledge, demonstrating for the first time that selective activation of sympathetic neurons originating in the SMG induces neurotransmitter release in the MLN and the spleen. Conditional expression of the activating optogenetic ChR2 coupled in sympathetic neurons with a spatially restricted illumination system to deliver 465 nm light provides a highly selective system to excite cell bodies in the peripheral sympathetic ganglia. Application of stimulation to the SMG resulted in the release of NE and ACh in the MLN, and in the spleen. Using a selective β2AR antagonist prior to neural stimulation we demonstrated a requirement for NE acting through β2AR to induce ACh release in the spleen, as neural stimulation in the presence of ICI 118 551 increased NE without a corresponding increase in ACh. These data would indicate that evoked release of NE precedes ACh in a β2AR dependent manner *in vivo.* Our data are in agreement with prior literature demonstrating β2AR expression on T-cells, and experiments indicating a role for these receptors resulted in the CAIP (3, 30, 38, 39). These findings suggest that sympathetic induction of ACh release from $ChAT^{+}$ T-cells resulting in the regulation of immune cell activity is a generalized mechanism of immune control in a variety of lymphoid tissues.

It should also be noted that there is considerable contextual and possibly circuit dependent effects in neuronal control of immune responses. For example, activation of the sympathetic nervous system and consequently the release of NE can be pro-inflammatory, or anti-inflammatory and can induce pro-restitutive effects (40–43). At this point it appears there could be two or more discrete anti-inflammatory pathways that can down regulate immune cell activation through sympathetic nerve fibers that project to secondary lymphoid organs. In addition to the CAIP, it is clear that selective stimulation of the afferent vagal pathway induces an anti-inflammatory response due to sympathetic activation indicated by action potentials generated in splenic projecting sympathetic fibers (9, 44). This discrete splanchnic anti-inflammatory pathway reduces LPS-induced inflammation independent of the nicotinic α7 receptor, highlighting that this is unique from the CAIP (45). Understanding how each of these circuits can contribute to control over aberrant immune cell activation will be essential in leveraging this knowledge for therapeutics.

Innervation of lymph nodes has been described in several animal species including rats, mice, hamster and cats. As in the spleen of mice (46), and in agreement with the literature (47), we did not observe cholinergic innervation within the MLN of ChAT-GFP$^+$ mice. Confocal analysis of MLN sections revealed sympathetic innervation indicated by TH$^+$ fibers were sparse and primarily localized to the hillus of the MLN and appeared to be associated with the vasculature. These data contrast with the literature, where abundant sympathetic innervation in MLN of NZW mice was described. While no direct comparison between mouse strains have been performed, sparse innervation has been noted in the literature (20). Highlighting strain differences in the sympathetic innervation of secondary lymphoid organs, chemical sympathectomy significantly reduced B-cell responses in NZW but not C57BL/6 mice (18). These data suggest that there could be significant strain differences in sympathetic innervation of lymph nodes. While we and others have observed the presence of ChAT$^+$ B-cells within spleen and MLN (16, 17, 48), it is important to note that unlike ChAT$^+$ T-cells these cells do not release ACh in response to NE (16). Therefore, selective activation of sympathetic neurons projecting to the MLN would seem unlikely to induce ACh release from ChAT$^+$ B-cells. Our data indicate that close contact between axons and ChAT$^+$ T-cells are not likely required, and that NE signaling to this target cell population can occur without synapse-like connections (17).

Although targeted stimulation of conditionally expressed ChR2 in the SMG revealed communication to the MLN and spleen, these data could be indicative of a sympathetic neuroinhibitory pathway that is independent of the vagus nerve. Indeed a sympathetic inhibitory circuit has recently been described whereby splanchnic nerve activates an anti-inflammatory response in a variety of abdominal organs to reduce LPS-induced TNFα production (49). To determine if VNS induced NE and ACh release in the spleen through the SMG, we performed halorhodopsin-mediated neural inhibition targeted to the SMG during VNS. As previously reported, VNS induced significant increases in concentration of NE and ACh released in the spleen (3), that was blocked by halorhodopsin mediated neuronal inhibition concurrent to electrical stimulation of the vagus. We further identified that optogenetic blockade applied at the SMG during VNS was sufficient to restore LPS-induced TNFα production. These findings indicate that the SMG is a critical node in the functional circuit to the MLN and spleen elicited by VNS, and this contention is supported by prior

neuroanatomical mapping studies (6, 7). We further verified that activation of this portion of the efferent reflex arc not only increased NE and ACh in the spleen, but that optogenetic activation of TH^+ neurons in the SMG was sufficient to significantly reduce LPS-induced TNFα production.

Although prior elegant studies using VNS applied distal to a transection of the cervical vagus demonstrated retained functional immune inhibition, it has been uncertain as to what anatomical connections there are between the efferent vagus and lymphoid organs. These early studies in rats demonstrated that injection of the dye DiI into the DMN, resulted in the labeling of vagal efferents within the SMG and celiac ganglia (6). It is important to note that this proposed neuroanatomy remains contentious, given recent failures to reproduce this pathway. In particular, injection of DiI in the DMN and fast blue in the spleen did not result in co-localization of these two tracers in the superior mesenteric/celiac ganglia, and electrical VNS did not induce splenic nerve activity in rats (9).

Further highlighting the importance of additional neuroanatomical and functional studies, there is evidence supporting, and refuting the indirect innervation of the spleen in studies using PRV-mediated circuit tracing. Direct intrasplenic injection of the PRV Bartha strain resulted in viral labeling of the intermediolateral cell column (IML) of the spinal cord, and DMN. This propagation to the DMN however was absent in mice previously subjected to sub-diaphragmatic vagotomy, suggesting that the virus has entered the DMN through vagal efferent fibers (10). These data contradict prior observations where intrasplenic injection of the same PRV strain resulted in infection of neurons in the DMV that was attributed to projections from other infected brain regions as opposed to evidence of a vagal efferent to spleen neural circuit (11).

It is conceivable that these conflicting results in the literature are due to the presence of two or more neuroanatomical pathways that converge in sympathetic ganglia to affect immunological processes. Evidence of multiple neuroanatomical pathways that can be initiated by neural stimulation have been demonstrated in delineating the pathway for stress-induced anti-inflammatory pathway that is protective during ischemia reperfusion injury (IRI) of the kidney (30). Although activation of C1 neurons in the brainstem result in vagal nerve activity, and reduced IRI, animals previously subjected to sub-diaphragmatic vagotomy exhibited equivalent protection from IRI (30). These data along with electrophysiological recording from the renal sympathetic nerve and loss of protective effect with the ganglionic blocker hexamethonium, suggest that a parallel canonical sympathetic pathway provided protection (30).

As the sympathetic mesenteric nerve that provides sympathetic innervation to the intestinal tract originates in the SMG, it is conceivable that stimulation of this nerve could induce activation of the MLN innervation. Prior studies have focused on the spleen or the intestinal tract as the sites of action, without considering the effect on other secondary lymphoid organs that can induce regional immune responses. In the intestine, VNS has proven efficacious at significantly reducing inflammation in the Trinitrobenzenesulfonic acid (TNBS)-induced model of colitis (50, 51). Activation of the efferent arm of the CAIP in mice with the acetylcholinesterase inhibitor galantamine or the muscarinic M1 receptor

agonist MCN-A-543 has also been shown to significantly reduce the severity of dextran sulfate sodium (DSS)-induced colitis. Reduced colitis severity with galantamine treatment was further shown to be dependent on an intact vagus and splenic nerve and was associated with reduced maturation of splenic $CD11c^+$ DC (52). Although these groundbreaking studies highlighted the ability of the CAIP to modulate intestinal inflammation, the effect on the MLN as inductive sites for the intestine were not established. This regulation of intestinal inflammation through the vagus has been well established, with loss of tonic vagal nerve signaling by surgical vagotomy significantly enhancing the severity of DSS-induced colitis (53–55). Inhibition of colitis is not restricted to the DSS model, with VNS significantly reducing colitis induced by oxazolone (56). These recent findings suggest that VNS can limit aberrant activation of a variety of immune cells beyond macrophages, consequently reducing induced colonic inflammation.

Once again highlighting that a parallel sympathetic anti-inflammatory pathway exists, direct stimulation of the superior mesenteric nerve reduced macroscopic disease parameters in DSS-induced colitis. These studies further identified that ablation of vagal innervation to the intestine had no effect on the severity of DSS-induced colitis (43). Although these studies indicate that the colonic mucosa is not a direct target of VNS, our findings suggest that activation of the efferent arm of the CAIP, or direct activation of the SMG could result in inhibition of immune responses in the lymph nodes draining the intestinal tract. Blockade of immune cell activation within these tissues could prove to be another important site of action in this treatment modality.

Given the tremendous clinical interest and ongoing clinical trials using VNS in the treatment of IBD, these questions pertaining to functional circuitry are timely and pertinent. Clinical trials of implanted VNS devices resulted in significant improvement in 5 of 7 patients with active moderate Crohn’s disease at enrollment (13). Interestingly, patients refractive to this therapy had increased severity of disease at the time of enrollment. It is uncertain if failure to control inflammation was simply a product of increased initial disease severity, or a result of reduced sympathetic signaling during inflammation coupled with alterations to the functional neuronal circuitry (57, 58). It is also conceivable that as this trial identified a latency of treatment effect (13), that control of inflammation occurs not just in the mucosa, but also in the immune inductive sites such as the MLN. There is a significant amount of work to be done in the precise mapping of these functional neuro-immune circuits, both in health and during chronic inflammation, that are being enabled by novel technologies including optogenetics. Our studies identify the SMG as a novel target that not only functions as a node in the CAIP but could be used to induce activation of sympathetic innervation of the spleen and MLN.

Supplementary Material

Refer to Web version on PubMed Central for supplementary material.

Acknowledgements:

This work was funded in part by an NIH grant to CR (OT2 OD023871), and KM was funded in part by a NIGMS-funded Pharmacology Training Program grant (T32GM099608).

References Cited

1. Borovikova LV, et al. (2000) Vagus nerve stimulation attenuates the systemic inflammatory response to endotoxin. Nature 405(6785):458–462. [PubMed: 10839541]
2. Wang H, et al. (2003) Nicotinic acetylcholine receptor [alpha]7 subunit is an essential regulator of inflammation. Nature 421(6921):384–388. [PubMed: 12508119]
3. Rosas-Ballina M, et al. (2011) Acetylcholine-Synthesizing T Cells Relay Neural Signals in a Vagus Nerve Circuit. Science.
4. Reardon C, Murray K, & Lomax AE (2018) Neuroimmune Communication in Health and Disease. Physiological Reviews 98(4):2287–2316. [PubMed: 30109819]
5. Rosas-Ballina M, et al. (2008) Splenic nerve is required for cholinergic antiinflammatory pathway control of TNF in endotoxemia. Proceedings of the National Academy of Sciences 105(31):11008–11013.
6. Berthoud HR & Powley TL (1993) Characterization of vagal innervation to the rat celiac, suprarenal and mesenteric ganglia. J Auton Nerv Syst 42(2):153–169. [PubMed: 8450174]
7. Nance DM & Burns J (1989) Innervation of the spleen in the rat: Evidence for absence of afferent innervation. Brain Behav Immun 3(4):281–290. [PubMed: 2611414]
8. Olofsson YAL PS, Caravaca A, Chavan SS, Pavlov VA, Faltys M, Tracey KJ. (2015) Single-Pulse and Unidirectional Electrical Activation of the Cervical Vagus Nerve Reduces Tumor Necrosis Factor in Endotoxemia. Bioelectronic Medicine 2:37–42.
9. Bratton BO, et al. (2012) Neural regulation of inflammation: no neural connection from the vagus to splenic sympathetic neurons. Exp Physiol 97(11):1180–1185. [PubMed: 22247284]
10. Buijs RM, van der Vliet J, Garidou M-L, Huitinga I, & Escobar C (2008) Spleen Vagal Denervation Inhibits the Production of Antibodies to Circulating Antigens. PLOS ONE 3(9):e3152. [PubMed: 18773078]
11. Cano G, Sved AF, Rinaman L, Rabin BS, & Card JP (2001) Characterization of the central nervous system innervation of the rat spleen using viral transneuronal tracing. J Comp Neurol 439(1):1–18. [PubMed: 11579378]
12. Koopman FA, et al. (2016) Vagus nerve stimulation inhibits cytokine production and attenuates disease severity in rheumatoid arthritis. Proc Natl Acad Sci USA 113(29):8284–8289. [PubMed: 27382171]
13. Bonaz B, et al. (2016) Chronic vagus nerve stimulation in Crohn's disease: a 6-month follow-up pilot study. Neurogastroenterol Motil 28(6):948–953. [PubMed: 26920654]
14. Houston SA, et al. (2015) The lymph nodes draining the small intestine and colon are anatomically separate and immunologically distinct. Mucosal Immunology 9:468. [PubMed: 26329428]
15. Nance DM & Sanders VM (2007) Autonomic Innervation and Regulation of the Immune System (1987–2007). Brain Behav Immun 21(6):736–745. [PubMed: 17467231]
16. Reardon C, et al. (2013) Lymphocyte-derived ACh regulates local innate but not adaptive immunity. Proceedings of the National Academy of Sciences of the United States of America.
17. Murray K, et al. (2017) Neuroanatomy of the spleen: Mapping the relationship between sympathetic neurons and lymphocytes. PLOS ONE 12(7):e0182416. [PubMed: 28753658]
18. Felten DL, et al. (1984) Sympathetic innervation of lymph nodes in mice. Brain Research Bulletin 13(6):693–699. [PubMed: 6532515]
19. Popper P, Mantyh CR, Vigna SR, Maggio JE, & Mantyh PW (1988) The localization of sensory nerve fibers and receptor binding sites for sensory neuropeptides in canine mesenteric lymph nodes. Peptides 9(2):257–267.
20. Carlson SL, et al. (1995) NGF modulates sympathetic innervation of lymphoid tissues. J Neurosci 15(9):5892–5899. [PubMed: 7666174]
21. Panuncio AL, De La Pena S, Gualco G, & Reissenweber N (1999) Adrenergic innervation in reactive human lymph nodes. J Anat 194 (Pt 1):143–146. [PubMed: 10227676]
22. Kurkowski R, Kummer W, & Heym C (1990) Substance P-immunoreactive nerve fibers in tracheobronchial lymph nodes of the guinea pig: origin, ultrastructure and coexistence with other peptides. Peptides ll(l):13–20.

23. Bilski AJ, Halliday SE, Fitzgerald JD, & Wale JL (1983) The pharmacology of a beta 2-selective adrenoceptor antagonist (ICI 118,551). Journal of cardiovascular pharmacology 5(3):430–437. [PubMed: 6191142]
24. Spandidos A, Wang X, Wang H, & Seed B (2010) PrimerBank: a resource of human and mouse PCR primer pairs for gene expression detection and quantification. Nucleic Acids Research 38(Database issue):D792–D799. [PubMed: 19906719]
25. Bankhead P, et al. (2017) QuPath: Open source software for digital pathology image analysis. Scientific Reports 7(1):16878. [PubMed: 29203879]
26. Wang X, et al. (2003) Up-regulation of secretory leukocyte protease inhibitor (SLPI) in the brain after ischemic stroke: adenoviral expression of SLPI protects brain from ischemic injury. Mol Pharmacol 64(4):833–840. [PubMed: 14500739]
27. Levine YA, et al. (2014) Neurostimulation of the cholinergic anti-inflammatory pathway ameliorates disease in rat collagen-induced arthritis. PLoS One 9(8):el04530.
28. Gigliotti JC, et al. (2015) Ultrasound Modulates the Splenic Neuroimmune Axis in Attenuating AKI. Journal of the American Society of Nephrology: JASN 26(10):2470–2481. [PubMed: 25644106]
29. Inoue T, et al. (2016) Vagus nerve stimulation mediates protection from kidney ischemia-reperfusion injury through α7nAChR+ splenocytes. The Journal of Clinical Investigation 126(5): 1939–1952. [PubMed: 27088805]
30. Abe C, et al. (2017) Cl neurons mediate a stress-induced anti-inflammatory reflex in mice. Nat Neurosci 20(5):700–707. [PubMed: 28288124]
31. Matteoli G, et al. (2014) A distinct vagal anti-inflammatory pathway modulates intestinal muscularis resident macrophages independent of the spleen. Gut 63(6):938–948. [PubMed: 23929694]
32. Berthoud HR, Carlson NR, & Powley TL (1991) Topography of efferent vagal innervation of the rat gastrointestinal tract. Am J Physiol 260(1 Pt 2):R200–207. [PubMed: 1992820]
33. Bogunovic M, et al. (2009) Origin of the lamina propria dendritic cell network. Immunity 31(3): 513–525. [PubMed: 19733489]
34. Hart AL, et al. (2005) Characteristics of intestinal dendritic cells in inflammatory bowel diseases. Gastroenterology 129(1):50–65. [PubMed: 16012934]
35. Malmstrom V, et al. (2001) CD134L expression on dendritic cells in the mesenteric lymph nodes drives colitis in T cell-restored SCID mice. J Immunol 166(11):6972–6981. [PubMed: 11359859]
36. Worbs T, Hammerschmidt SI, & Forster R (2016) Dendritic cell migration in health and disease. Nature Reviews Immunology 17:30.
37. Cummings RJ, et al. (2016) Different tissue phagocytes sample apoptotic cells to direct distinct homeostasis programs. Nature 539:565. [PubMed: 27828940]
38. Riether C, et al. (2011) Stimulation of beta(2)-adrenergic receptors inhibits calcineurin activity in CD4(+) T cells via PKA-AKAP interaction. Brain Behav Immun 25(1):59–66. [PubMed: 20674738]
39. Guereschi MG, et al. (2013) Beta2-adrenergic receptor signaling in CD4+ Foxp3+ regulatory T cells enhances their suppressive function in a PKA-dependent manner. Eur J Immunol 43(4):1001–1012. [PubMed: 23436577]
40. Gabanyi I, et al. (2016) Neuro-immune Interactions Drive Tissue Programming in Intestinal Macrophages. Cell 164(3):378–391. [PubMed: 26777404]
41. Pongratz G & Straub RH (2012) Role of peripheral nerve fibres in acute and chronic inflammation in arthritis. Nature Reviews Rheumatology 9:117. [PubMed: 23147892]
42. Straub RH, et al. (2008) Anti-inflammatory role of sympathetic nerves in chronic intestinal inflammation. Gut 57(7):911–921. [PubMed: 18308830]
43. Willemze RA, et al. (2017) Neuronal control of experimental colitis occurs via sympathetic intestinal innervation. Neurogastroenterology & Motility:e13163–n/a.
44. Komegae EN, et al. (2018) Vagal afferent activation suppresses systemic inflammation via the splanchnic anti-inflammatory pathway. Brain Behav Immun 73:441–449. [PubMed: 29883598]

45. Vida G, Pena G, Deitch EA, & Ulloa L (2011) alpha7-cholinergic receptor mediates vagal induction of splenic norepinephrine. J Immunol 186(7):4340–4346. [PubMed: 21339364]
46. Bellinger DL, Lorton D, Hamill RW, Felten SY, & Felten DL (1993) Acetylcholinesterase staining and choline acetyltransferase activity in the young adult rat spleen: lack of evidence for cholinergic innervation. Brain Behav Immun 7(3):191–204. [PubMed: 8219410]
47. Schafer MK, Eiden LE, & Weihe E (1998) Cholinergic neurons and terminal fields revealed by immunohistochemistry for the vesicular acetylcholine transporter. II. The peripheral nervous system. Neuroscience 84(2):361–376. [PubMed: 9539210]
48. Dhawan S, et al. (2016) Acetylcholine producing T-cells in the intestine affect antimicrobial peptide expression and microbial diversity. American Journal of Physiology - Gastrointestinal and Liver Physiology.
49. Martelli D, Farmer DGS, McKinley MJ, Yao ST, & McAllen RM (2019) Anti-inflammatory reflex action of splanchnic sympathetic nerves is distributed across abdominal organs. Am J Physiol Regul Integr Comp Physiol 316(3):R235–R242. [PubMed: 30576218]
50. Meregnani J, et al. (2011) Anti-inflammatory effect of vagus nerve stimulation in a rat model of inflammatory bowel disease. Auton Neurosci 160(1–2):82–89. [PubMed: 21071287]
51. Sun P, et al. (2013) Involvement of MAPK/NF-kappaB signaling in the activation of the cholinergic anti-inflammatory pathway in experimental colitis by chronic vagus nerve stimulation. PLoS One 8(8):e69424. [PubMed: 23936328]
52. Munyaka P, et al. (2014) Central muscarinic cholinergic activation alters interaction between splenic dendritic cell and CD4+CD25-T cells in experimental colitis. PLoS One 9(10):e109272. [PubMed: 25295619]
53. O'Mahony C, van der Kleij H, Bienenstock J, Shanahan F, & O'Mahony L (2009) Loss of vagal anti-inflammatory effect: in vivo visualization and adoptive transfer. Am J Physiol Regul Integr Comp Physiol 297(4):R1U8–U26. [PubMed: 19439616]
54. Ghia J- E, Blennerhassett P, & Collins SM (2007) Vagus nerve integrity and experimental colitis. American Journal of Physiology - Gastrointestinal and Liver Physiology 293(3):G560–G567. [PubMed: 17585014]
55. Ghia JE, Blennerhassett P, Kumar-Ondiveeran H, Verdu EF, & Collins SM (2006) The vagus nerve: a tonic inhibitory influence associated with inflammatory bowel disease in a murine model. Gastroenterology 131(4):1122–1130. [PubMed: 17030182]
56. Meroni E, et al. (2018) Functional characterization of oxazolone-induced colitis and survival improvement by vagus nerve stimulation. PLoS One 13(5):e0197487. [PubMed: 29791477]
57. Motagally MA, Lukewich MK, Chisholm SP, Neshat S, & Lomax AE (2009) Tumour necrosis factor alpha activates nuclear factor kappaB signalling to reduce N-type voltage-gated Ca2+ current in postganglionic sympathetic neurons. J Physiol 587(Pt 11):2623–2634. [PubMed: 19403618]
58. Motagally MA, Neshat S, & Lomax AE (2009) Inhibition of sympathetic N-type voltage-gated Ca2+ current underlies the reduction in norepinephrine release during colitis. American journal of physiology. Gastrointestinal and liver physiology 296(5):G1077–1084. [PubMed: 19264956]

Highlights:

- Mesenteric lymph nodes and spleen are innervated by the sympathetic nervous system
- This innervation can be selective activated
- Selective neuronal activation significantly reduces pro-inflammatory cytokine expression

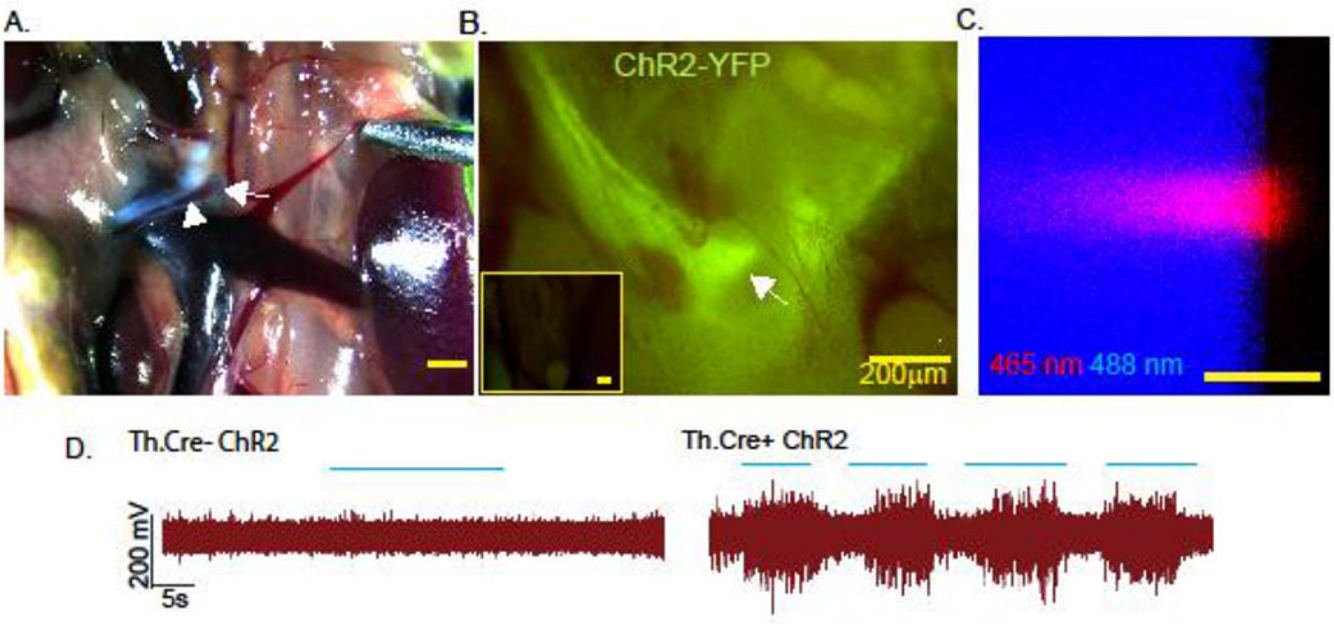

Fig. 1. Site specific peripheral neuronal activation by optogenetics.

The superior mesenteric ganglion (arrow) was identified using the superior mesenteric nerve (arrowheads) as an anatomical landmark under a brightfield stereodissection microscope **(A).** YFP expression was detected in Th.Cre^{+} ChR2-YFP^{LSL} but not Th.Cre- ChR2-YFP^{LSL} mice (inset) was assessed using a stereo-epifluorescence microscope with a YFP bandpass filter **(B).** Characterization of the size of light emitted from the fiberoptic patch cable by confocal microscopy using on edge illumination of a plexiglass slide. Boundaries of the slide are revealed using 488 nm laser light excitation from the microscope **(C).** Optogenetic stimulation (blue lines indicate “pulses of light”) of the SMG results in compound action potentials in the superior mesenteric nerve of Th.cre+ ChR2 but not Th.Cre- ChR2 mice **(D).** Images and electrical recordings are representative of 3–4 mice, or 3 separate experiments in the case of “B”.

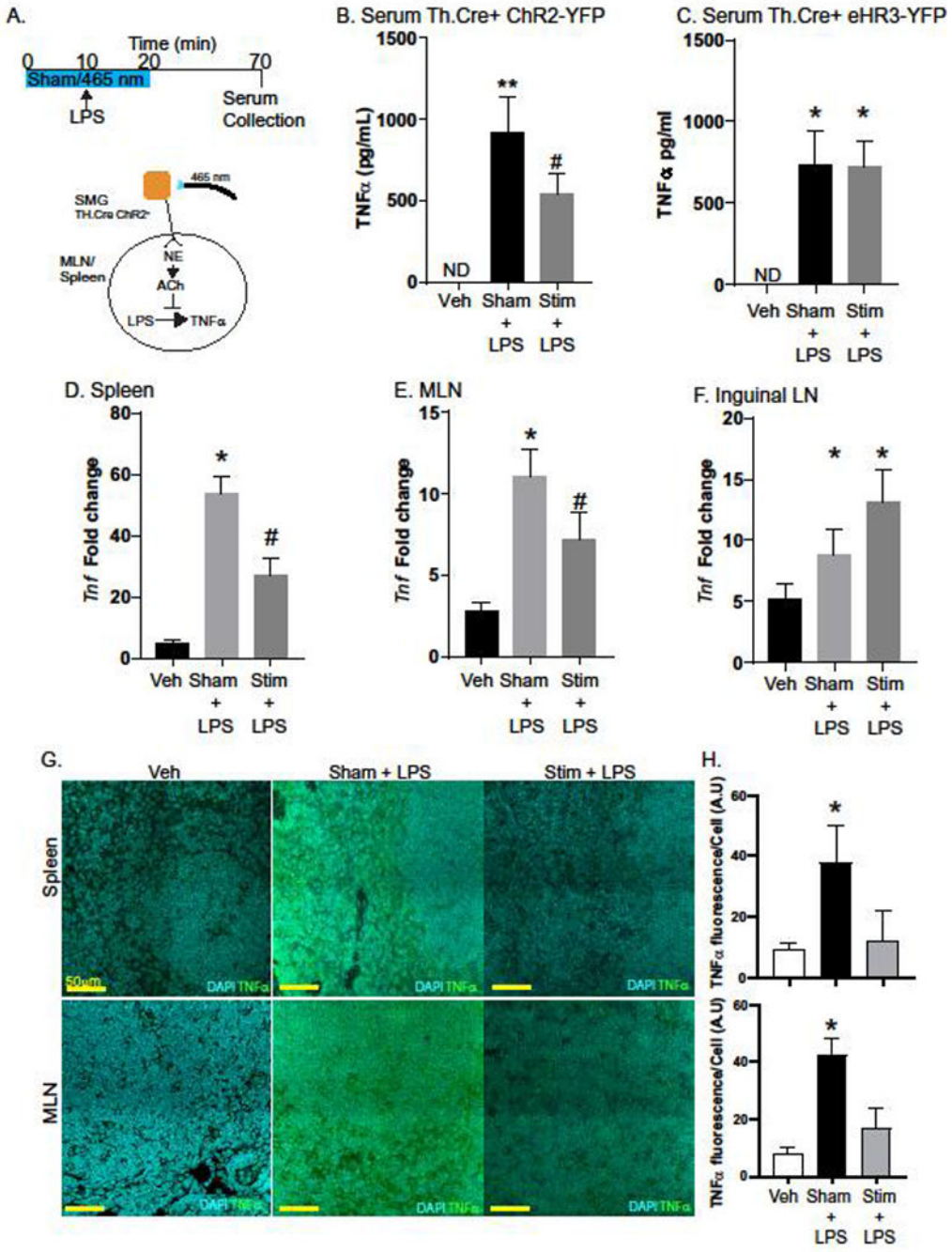

Fig. 2. Activation of sympathetic neurons in the SMG blocks LPS-induced TNFα production.

To test the ability of sympathetic neurons in the SMG to regulate LPS-induced TNFα production, *a* conditional optogenetic approach was used. After exposure of the SMG, mice were either subjected to sham (no light) or 465 nm light pulses for 10 minutes prior to i.v. injection of LPS (4 mg/kg) and continued for a total of 20 minutes (Stim). Vehicle control mice received sterile PBS (i.v.) **(A).** Serum collected revealed LPS induced TNFα production was significantly lower in stimulated (ChR2) vs. Sham treated mice **(B).** Mice that express the inhibitory halorhodopsin-YFP did not exhibit 465 nm induced reductions in

TNFα production **(C).** Expression of TNFα mRNA was significantly reduced in ChR2 stimulated LPS treated mice compared to Sham in the spleen **(D)** and MLN **(E)** but not the inguinal LN **(F).** Tissues from these mice were evaluated by confocal microscopy **(G)** to determine TNFα production by fluorescence per DAPI+ cell **(H).** n= 5–8 mice/group in 2 experiments with #, * $P<0.05$ ANOVA Tukey post-test compared to all groups. ND= none detected, data are presented as mean ± SEM for all panels. qPCR results are fold expression normalized to control and the endogenous *Actb* gene as described in the methods.

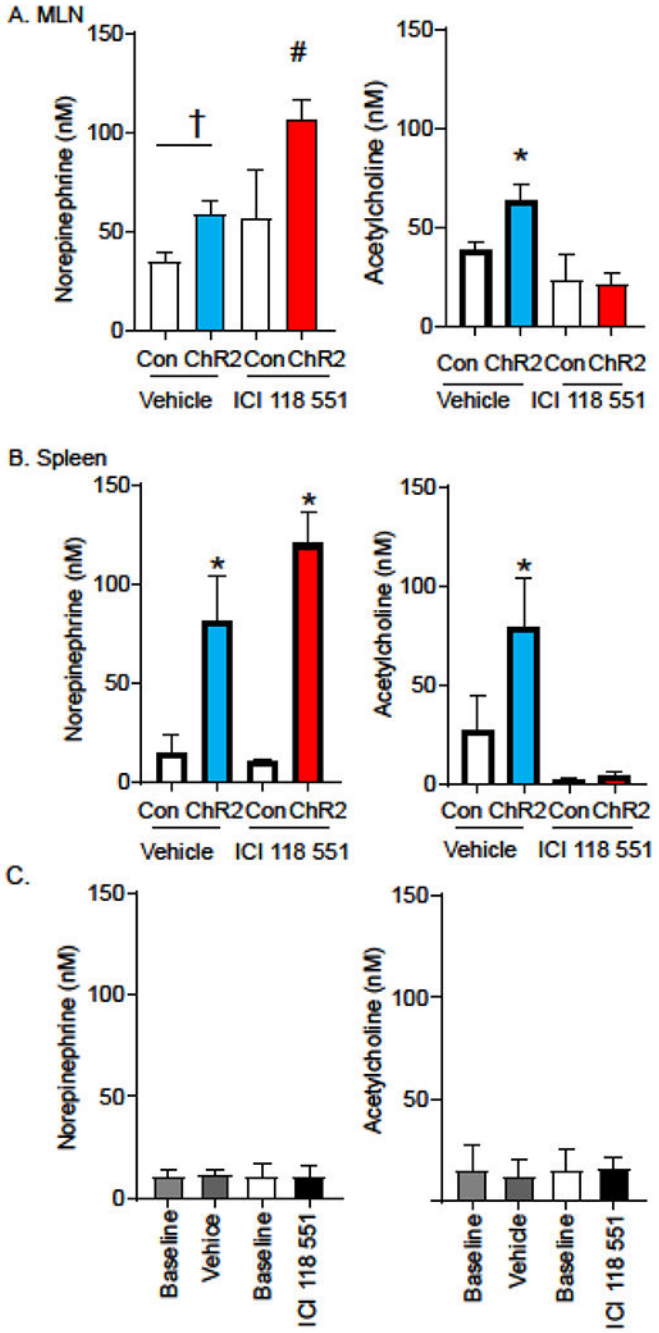

Fig 3. Optogenetic stimulation of sympathetic neurons in the SMG induces β2AR dependent Ach release in MLN and spleen.

Stimulation of sympathetic neurons expressing ChR2 in the SMG induces the release of NE in the MLN **(A, left panel)** and spleen **(B left panel)** of mice treated with vehicle **(blue bars)** or the highly selective β2AR antagonist ICI 118 551 **(red bars).** While stimulation evokes ACh release in the MLN and spleen of vehicle treated mice **(blue bars),** no increase in ACh is detected in the animals treated with ICI 118 551 **(red bars, A** & **B, right panel).** In a separate cohort of animals, we compared NE and ACh released before (baseline) and

after i.v. injection of vehicle or ICI 118 551 (C). n= 6–10 mice per group in 3 experiments, †P<0.05 between indicated groups, #,* P <0.05, between all other groups, ANOVA Tukey post-test, data are presented as mean ± SEM for all panels.

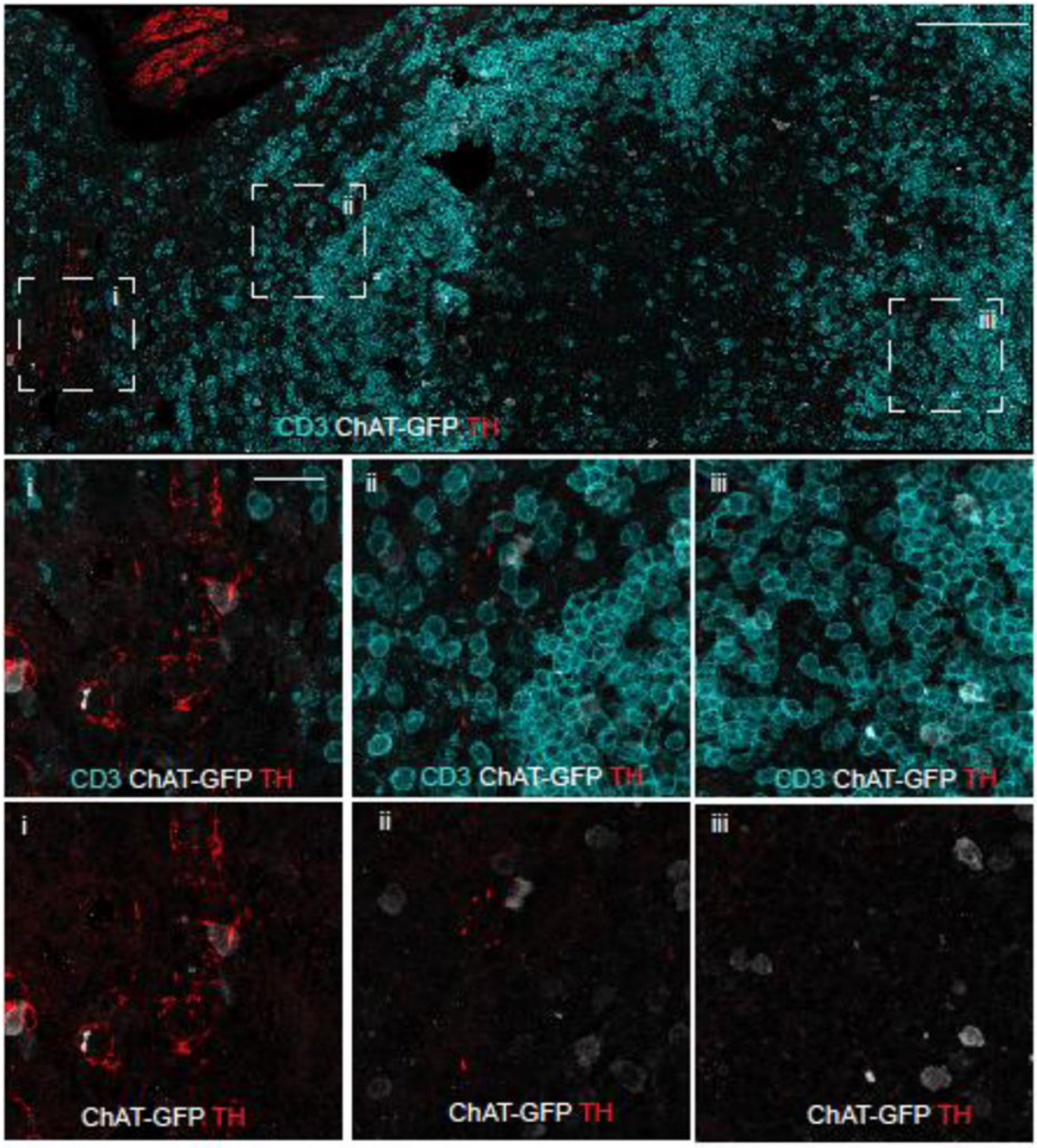

Fig 4. Sympathetic innervation is sparse in the MLN.

Confocal microscopy was conducted on tissue sections ChAT-GFP (C57BL/6 background) mice for T-cells (anti-CD3), ChAT (anti-GFP), and sympathetic axons (anti-TH). The section was identified and overlapping tiles were acquired from 943 μm x 454 μm area of MLN (upper panel, scale bar =100 μm). Areas indicated in the bounding boxes are shown in the middle (CD3, ChAT-GFP, TH) and lower panels (ChAT-GFP, TH, scale bar = 20 μm). Region of the hilus in the MLN is within box “i”. Representative images obtained from 8 mice.

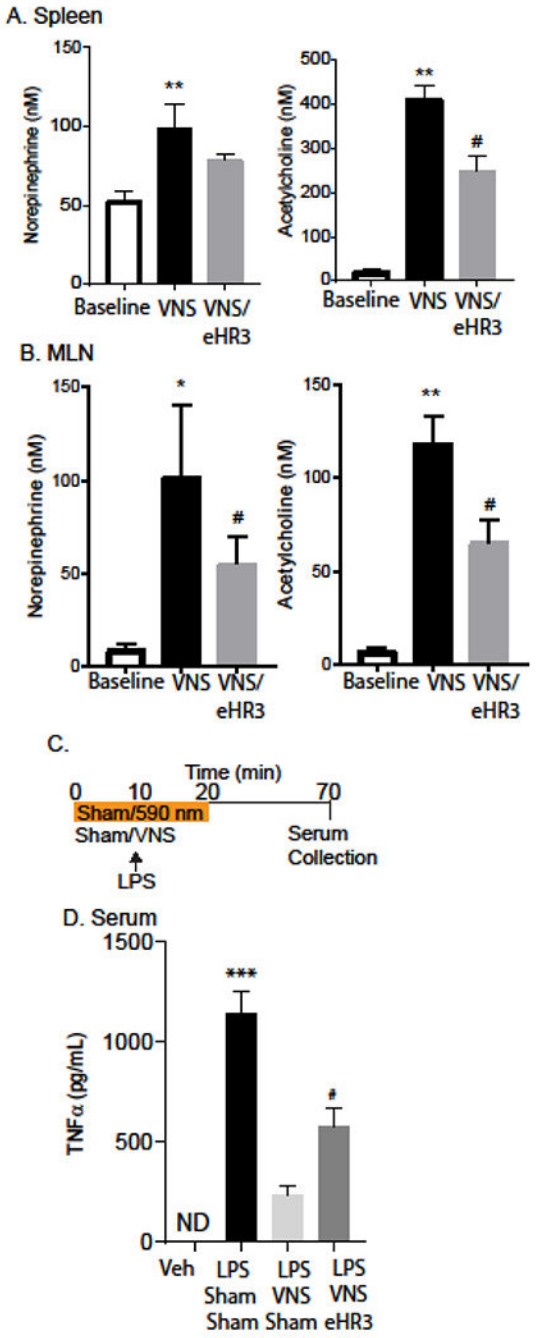

Fig. 5. Optogenetic mediated blockade reduces electrical VNS induced release of neurotransmitters in the MLN and spleen.

Mice expressing the inhibitory eHR3 halorhodopsin in sympathetic neurons (Th.Cre eHR3^{+}) were subjected to electrical stimulation of the left cervical vagus nerve with or without concurrent halorhodopsin mediated neuronal blockade. Mass spectrometry was conducted on the microdialysate for NE (left) and ACh (right) from the spleen **(A)** and MLN **(B).** n=8 mice/group in two experiments ** P<0.001, *,# P<0.05, ANOVA, Tukey post hoc–test. Th.Cre eHR3 animals were then challenged with LPS and subject to either VNS treatment only or VNS and inhibitory eHR3 SMG stimulation **(C).** Serum was collected and analyzed

via ELISA for TNFα **(D).** n= 6–8 mice/group in two experiments ***P<0.0001, #P<0.05, ANOVA, Tukey post–hoc test, data are presented as mean ± SEM.